PROCEEDINGS OF SCIENCE

GERDA Phase II first commissioning results and future prospectives for neutrinoless double beta decay

Carla Macolino* for the GERDA collaboration†
Laboratori Nazionali del Gran Sasso and Gran Sasso Science Institute, INFN Italy
E-mail: carla.macolino@lngs.infn.it

The GERmanium Detector Array (GERDA) searches for neutrinoless double beta decay ($0\nu\beta\beta$) of ^{76}Ge. The experiment has already completed the Phase I reaching an unprecedent low level of background and establishing a limit on the half-life of the decay, $T_{1/2}^{0\nu\beta\beta} > 2.1 \cdot 10^{25}$ yr (at 90% C.L.). The second phase of the experiment is expected to start at the end of 2015, in which a larger mass of germanium detectors will be used and the background level will be lowered of a factor 10 thanks to the implementation of a LAr veto and the use of pulse-shape discrimination. For GERDA Phase II the projected sensitivity on the half-life is $T_{1/2}^{0\nu} \gtrsim 1.4 \cdot 10^{26}$ yr, after an exposure of about 100 kg·yr. In this paper the main results obtained from GERDA Phase I and the first commissioning results from Phase II are discussed.

XVI International Workshop on Neutrino Telescopes,
2-6 March 2015
Palazzo Franchetti, Istituto Veneto, Venice, Italy

*Speaker.
†http://www.mpi-hd.mpg.de/gerda

PoS(NEUTEL2015)050

1. Introduction

Neutrinoless double beta decay:

$$(A,Z) \rightarrow (A,Z+2) + 2e^- \tag{1.1}$$

is a process for atomic nuclei which violates lepton number conservation by two units. Observing such a decay would have fundamental consequences for the knowledge of the Majorana nature of the neutrino. The detection principle of GERDA is based on the use of bare high-purity (HPGe) germanium detectors isotopically enriched in ^{76}Ge (the enrichment fraction is about 86%) and immersed in liquid argon (LAr).
The experiment has completed the Phase I collecting an exposure of 21.6 kg·yr and reaching a background level with background index (BI) of the order of BI$\simeq 10^{-2}$ cts/(keV·kg·yr). No excess of events in the region around the expected peak from $0\nu\beta\beta$ decay has been detected and and a lower limit on the half-life of the decay has been determined: $\mathrm{T}^{0\nu}_{1/2} > 2.1 \cdot 10^{25}$ yr (90% C.L.). The collected data from Phase I have also been used to search for other ^{76}Ge decay modes like different Majoron accompanied decays.
At present the experiment is in its commissioning phase of the Phase II setup, in which the total mass of ^{76}Ge will be increased to about 35 kg and a veto based on the scintillation light from LAr will be implemented. This, in combination with an improved pulse-shape discrimination performance, will reduce the background by a factor of ten with respec to to Phase I. The projected sensitivity on half-life, after an exposure of 100 kg·yr and a background index of 10^{-3} cts/(keV·kg·yr), is $T^{0\nu}_{1/2} > 1.4 \cdot 10^{26}$ yr at 90% C.L.
In the following sections the main results from GERDA Phase I will be reviewed and the first commisioning data from GERDA Phase II will be presented. Finally, the prospectives for GERDA Phase II within the worldwide experimental scenario will be discussed.

2. The GERDA Phase I setup

Enriched germanium (^{enr}Ge) detectors of GERDA Phase I were arranged in strings and immersed in a cryostat filled with LAr. An artist view of the detector is shown in Fig. 1. The liquid argon acts as the cooling medium for the semiconductors and also as shield against external background. The internal side of the stainless steel cryostat vessel is covered with a copper lining to reduce gamma radiation from the cryostat walls. The central volume is separated by a 3 m high and 760 mm diameter cylinder made of 30 μm copper foil (called "radon shroud") to reduce convective transport of radon emanated from the vessel walls to the Ge diodes. The cryostat is surrounded by a large tank (8.5 m height and 10 m diameter) filled with 590 m^3 of ultra-pure water. The water tank is instrumented with 66 PMTs to detect Cherenkov light produced by muons. Muon veto is completed by an array of 36 plastic scintillator panels placed on the roof of the cleanroom. Cherenkov and scintillation signals are combined (according to a logic OR) as a muon veto for the data acquisition. A class 7 clean room and a two-arm lock are installed on the top of the GERDA building to insert the detectors into the cryostat. For additional details about the GERDA experimental setup see Ref. [1].
GERDA Phase I data taking started in November 2011 with 8 p-type ^{enr}Ge semi-coaxial detectors

PoS(NEUTEL2015)050

Figure 1: An artist's view of the GERDA detector. The array of Ge detectors is not to scale. (1): the array of germanium detector string; (2): the stainless steel cryostat; (3): copper lining; (4): the water tank; (5): the clean room; (6): the lock. Plot from Ref. [1].

(17.7 kg total mass), five of them from the previous Heidelberg-Moscow (HdM) experiment, and three from the IGEX experiment. A detector with natural isotope composition from the GENIUS-Test-Facility (3 kg) was also implemented. In July 2012, five Broad Energy Germanium detectors (BEGe), with total mass of 3.6 kg, were added in the cryostat to test their performance in the GERDA environment. Signal was read out by charge sensitive amplifiers distant about 30 cm from the detectors and then digitized by 100 MHz Flash ADCs. Offline digital filters were used to reconstruct the physical parameters of interest, like energy and rise time of events [2]. The energy calibration was made every 1 or 2 weeks by irradiating the detectors with ^{228}Th sources. The average exposure-weighted energy resolution (FWHM) at $Q_{\beta\beta}$ is (4.8$\pm$0.2) keV for semi-coaxial detectors and (3.2$\pm$0.2) keV for BEGe detectors. Since a higher background level was observed when the BEGe detectors were inserted, Phase I data were divided into three sets; one containing the BEGe data (called "BEGe"), one containing semi-coaxial data taken in the period when the BEGe detectors were deployed (called "Silver") and the last containing the rest of the data from semi-coaxial detectors ("Golden"). Events in the region of interest (in the interval $Q_{\beta\beta}\pm$20 keV) were kept "blinded", *i.e.* not processed, until the calibration was finalized and all the selection cuts and analyses were fixed. The experimental energy spectrum from semi-coaxial and BEGe detectors was fitted to a background model in the range between 570 and 7500 keV: the fit result shows that the background is mainly due to sources located close to the detectors or on the detector surface and that the background in the region of interest is expected to be flat (see Ref. [3]). The interpolated value for the background index (BI) in the region of interest, with the exclusion of $\pm$5 keV around the expected position of the single escape peak from ^{208}Tl (2104 keV) and of the γ line from ^{214}Bi (2119 keV), BI=$1.75^{+0.26}_{-0.24}\times10^{-2}$ cts/(keV·kg·yr) for semi-coaxial detectors and BI=$3.6^{+1.3}_{-1.0}\times10^{-2}$ cts/(keV·kg·yr) for BEGe detectors. The characteristic shape of pulses from $0\nu\beta\beta$ events (electron events) was used to discriminate signal events from background ones (mainly gamma events or

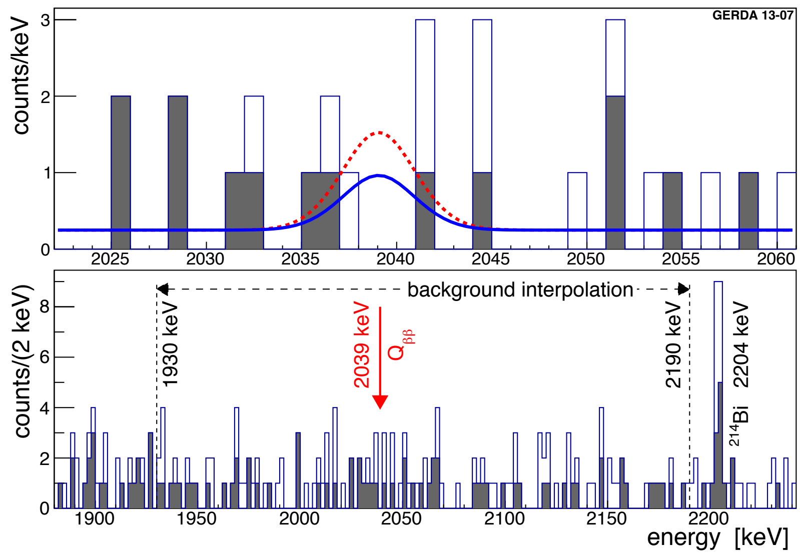

Figure 2: Energy spectrum from all ^{enr}Ge detectors with (filled) and without (open) PSD selection. In the upper panel, the expectation based on the central value of the half-life predicted by Ref. [7] is also shown (red), together with the 90% C.L. limit (blue). In the lower panel the energy window used for the background interpolation is indicated. Plot from Ref. [5].

events located in the surface). Different methods for Pulse Shape Discrimination (PSD) were considered for both semi-coaxial and BEGe detectors, according to the characteristics of the pulses and electric field distributions for the two types of detectors [4]. For a review of the GERDA experiment see also Ref. [6].

3. Results from GERDA Phase I

In this section the major results from GERDA Phase I data are discussed.

3.1 Limit on the half-life of $0\nu\beta\beta$ decay of ^{76}Ge

A limit on the half-life of $0\nu\beta\beta$ decay of ^{76}Ge was derived from GERDA Phase I data. After the collection of an exposure of 21.6 kg·yr (see Refs. [5] and [6]) the analysis cuts and methods were fixed, the region around $Q_{\beta\beta}\pm 5$ keV was unblinded. 7 events were observed while 5.1 ± 0.5 were expected from background. The Pulse Shape Discrimination cut rejected 3 out of 6 events from the semi-coaxial detectors and 1 from the BEGe detectors. The BI after the PSD cut on the “Golden” data set was 10^{-2} cts/(keV·kg·yr). No excess of events above the background expectation was observed. To derive the limit on signal counts $N^{0\nu}$ and the corresponding half-life $T^{0\nu}_{1/2}$, a profile likelihood fit of the three data sets was performed. The fitted function contained a constant term for the background and a Gaussian peak for the signal with mean at $Q_{\beta\beta}$ and standard deviation corrisponding to the energy resolution σ_E. The fitted parameters are the backgrounds of the three data sets and $1/T^{0\nu}_{1/2}$, which relates to the peak integral. The likelihood ratio was evaluated only for the physically allowed region in which $T^{0\nu}_{1/2} > 0$. The systematic uncertainties due to the detector parameters, selection efficiency, energy resolution and energy scale were folded in the fit with a Monte Carlo approach which takes correlations into account. The best fit value obtained was $N^{0\nu} = 0$ and the 90% C.L. limit is $N^{0\nu}$ <3.5 which translates in

$$T^{0\nu}_{1/2} > 2.1 \cdot 10^{25} \text{ yr (90\% C.L.)}, \tag{3.1}$$

which includes the systematic uncertainties. Given the background levels and the efficiencies, the median sensitivity for the 90 % C.L. limit was 2.4 $\cdot 10^{25}$ yr. In Fig. 2 the spectrum before and after PSD is shown together with the likelihood fit (solid blue curve) and the expectation based on the previous claim (dashed red curve from Ref. [7]) of $0\nu\beta\beta$ observation. Considering $T^{0\nu}_{1/2}$ from the claim in Ref. [7] at its face value, 5.9±1.4 decays would have been expected in $\Delta E = \pm 2\sigma_E$ and 2.0±0.3 background events after the PSD cuts (red dotted curve in Fig. 2). This was compared with the 3 events detected after the PSD cut, none of them within $Q_{\beta\beta} \pm \sigma_E$. The model ($H_1$) which includes the $0\nu\beta\beta$ signal calculated above, gives in fact a worse fit to the data than the background-only model (H_0): the Bayes factor, namely the ratio of the probabilities of the two models, is $P(H_1)/P(H_0)$ =0.024. Assuming the model H_1, the probability to obtain $N^{0\nu}$ =0 as the best fit from the profile likelihood analysis is P($N^{0\nu} = 0|H_1$)=0.01. The GERDA result therefore strongly disfavours the claim from Ref. [7] and it is consistent though stronger with the limits by the previous HdM [8] and IGEX [9] experiments. The profile likelihood fit was also extended to include the energy spectra from HdM and IGEX. Constant backgrounds for each of the five data sets and Gaussian peaks for the signal with common $1/T^{0\nu}_{1/2}$ are assumed. Experimental parameters (exposure, energy resolution, efficiency factors) were obtained from the original references or, when not available, extrapolated from the values used in GERDA. The best fit yields $N^{0\nu} = 0$ and a limit of

$$T^{0\nu}_{1/2} > 3.0 \cdot 10^{25} \text{ yr (90\% C.L.)}. \tag{3.2}$$

The Bayes factor in this case is $P(H_1)/P(H_0) = 2 \cdot 10^{-4}$; the claim of observation of $0\nu\beta\beta$ is even more strongly disfavored. The value of the combined half-life limit corresponds to an upper limits on the effective neutrino mass between 0.2 and 0.4 eV using different nuclear matrix element calculations.

3.2 Other physics results from GERDA Phase I

The GERDA collaboration has completed other interesting analyses on rare decays of ^{76}Ge: a new measurement of the half-life of the $2\nu\beta\beta$ process, the search for neutrinoless double beta decay of ^{76}Ge with Majoron emission and the search for $2\nu\beta\beta$ decay into excited states. The paper describing the first two analyses was submitted to EPJC [10], while the paper describing the search for two neutrino decays to excited states was submitted to J. Phys. G: Nucl. Phys. [11]. Finally, the GERDA collaboration has developped and tested a digital shaping filter with enhanced low-frequency rejection as an alternative to the standard Gaussian shaping used for energy reconstruction of GERDA data. Indeed, one of the crucial experimental parameters in the search for $0\nu\beta\beta$ decay is the energy resolution. The sensitivity to find a Gaussian peak over a flat background depends on the Full Width at Half Maximum (FWHM) at $Q_{\beta\beta}$ (2039 keV in the case of ^{76}Ge) as:

$$\mathrm{T}^{0\nu}_{1/2} \propto \frac{1}{\sqrt{\mathrm{FWHM}(\mathrm{Q}_{\beta\beta})}} \tag{3.3}$$

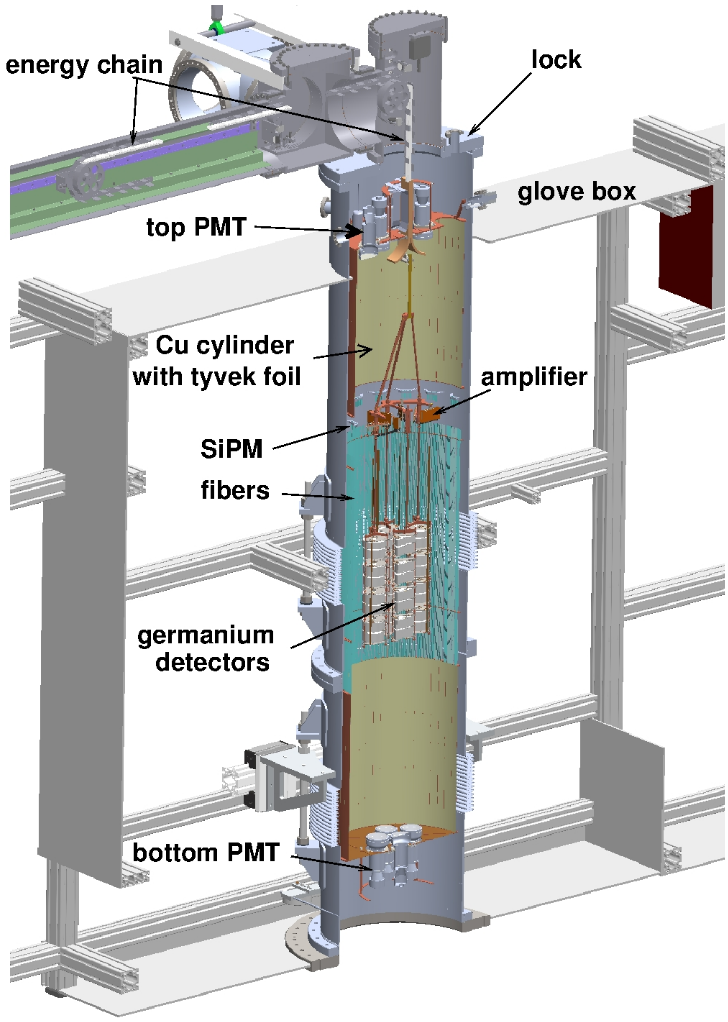

Figure 3: Design of the Phase II lock with the internal instrumentation.

where $T^{0\nu}_{1/2}$ is the sensitivity to give a limit for the $0\nu\beta\beta$ half-life at a given confidence level. During Phase I, the resolution was deteriorated due to low-frequency noise. The new filter consists in a cusp filter, which is known to be the optimum for series and parallel noise [12], if the filter has zero area, to reduce low-frequency noise [13] and if it has a central flat-top to correct of ballistic deficit. All Phase I calibration and physics data have been reprocessed, giving an average resolution improvement at $Q_{\beta\beta}$ of 0.3 keV for calibration data and about 0.5 keV for combined physics data. The same filter optimization technique will be used for Phase II data. Further details are described in Ref. [14].

4. On the way to Phase II: first commissioning results

GERDA Phase II will improve its sensitivity with respect to Phase I by a factor of 5-10 by increasing the detector mass and measurement time and reducing the background level by an order

Figure 4: Detector string with 4 pairs of BEGe detectors mounted and inserted in GERDA cryostat.

of magnitude. The background level can be lowered thanks to the detection of liquid argon scintillation light produced by ^{208}Tl or ^{214}Bi decays and by using pulse shape discrimination (PSD) techniques, which are more efficient for the the new detector type (BEGe detectors) implemented in Phase II. PSD allows, indeed, to discriminate surface events and multiple energy depositions in a detector with respect to single depositions made by emitted electrons from $0\nu\beta\beta$ decay.
Except for the cryostat and the muon veto, the other hardware components of GERDA Phase I have been replaced mostly during 2014. The Phase II setup is drawn in Fig. 3, where a cross section of the glove box (for detector handling in nitrogen atmosphere) and the lock together with the detectors, readout electronics, liquid argon veto and the energy chain are shown. The number of cables and feedthroughs for the readout of the germanium detector signals and the LAr veto increases by a factor of five compared to Phase I. Consequently the energy chain which carries all cables and is the support for detectors and veto, has a larger cross section and material thickness. The total radioactivity of the cables in the chain is similar compared to what achieved in Phase I being the specific radioactivity reduced thanks to a dedicated production. Radon emanation of 13 ± 4 mBq from the cables and the lock was measured with a 1 m^3 electrostatic radon monitor. This value is smaller than the emanation of the cryostat and the cryogenic infrastructure of 54 mBq.
The detector mass has been doubled with respect to Phase I by adding 30 BEGe type diodes made from material with ^{76}Ge fraction enriched to about 87%. Electrical contacts are made by wire bonding on aluminum pads which have been deposited on the detectors [15].
The mass of the materials surrounding the detectors has been reduced, being about 26 g for the copper used as the detector frame and 2 g for PTFE for insulation of the outer surface (in Phase I the copper frame weighted about 80 g and the PTFE spacers weighted about 11 g). About 40 g of ultrapure mono-cryostaline silicon is also used [16]. The first detectors were deployed in the GERDA cryostat soon after the new lock was installed and one entire string at the end of 2014 (see Fig. 4). Charge sensitive amplifiers for the readout of germanium detectors are placed, as in Phase

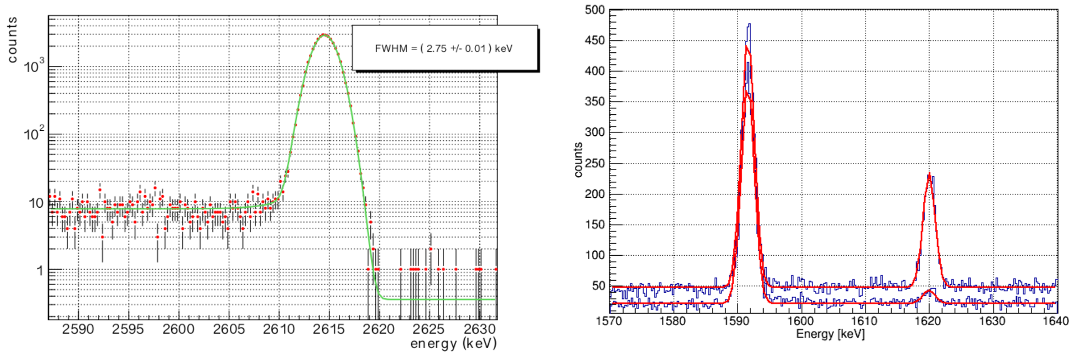

Figure 5: Left: ^{228}Th calibration spectrum at 2.6 MeV. Right: same spectrum around 1.6 MeV with and without PSD.

I, about 30 cm above the detectors. The long cables connecting the detectors to the amplifiers in Phase I were responsible for an increased sensitivity to microphonic noise. A zero area cusp digital filter sensitively reduces this noise (see Sec. 3.2, [14]).

The energy resolution and the result from the pulse shape discrimination technique from the string test data taking are shown in Fig. 5 for ^{228}Th calibration data. Detectors show an energy resolution of 2.8 keV (FWHM) at 2.6 MeV. For an acceptance of the double escape peak of ^{208}Tl (at 1592 keV) of 90%, about 13% of the ^{212}Bi peak events at 1621 keV survive after the PSD cut.

The liquid argon veto is made of a cylinder of 47 cm diameter and 2.2 m height which contains the detector array of strings of about 30 cm diameter and 40 cm height. Sixteen 3” PMTs (Hamamatsu R11065-20) are mounted at the top and bottom of the detector strings at a distance of about 80 cm (see Fig. 3). The central part of the cylinder is covered by a curtain of scintillating fibers (Bicron BCF-91A) whose collected light is read out by silicon photo multipliers (SiPM from Ketek). Two different views of the LAr veto are shown in Fig. 7. Fibers, PMTs and the cylindrical surface are covered with wavelenght shifter to shift the 128 nm scintillation light to about 400 nm where the quantum efficiency of the PMTs and SiPMs is at maximum.

At the start of Phase I an unexpected large background from ^{42}K (progeny of ^{42}Ar) was observed and eventually reduced to an acceptable level by encapsulating each detector string in a copper cylinder (called “mini-shroud”). This shroud is replaced in Phase II by a transparent nylon foil [17] covered with tetra-phenyl-buthadiene (TPB) to shift the 128 nm argon scintillation light to about 400 nm for the detection with PMTs and SiPM.

The effect of the nylon foil and PSD for ^{42}K surface β decays is shown in Fig. 6, for data taken from a measurement in the LArGe cryostat [18] filled with argon enriched in ^{42}Ar. Depending on the PSD performance, the Phase II background is expected to be dominated by this source at a level close to 0.001 cts/(keV·kg·yr). The suppression performance of the LAr veto is shown in Fig. 8, where the energy spectrum (from 2 depleted and 1 enriched BEGe detectors of the commissioning string) irradiated with a ^{228}Th calibration source is drawn, for a total statistics of 15 hours. In this configuration 16 out of 16 PMTs were working while only 7 out of 15 SiPM were operational. The plot shows the spectrum before any cut, the spectrum after PSD only, the spectrum after LAr scin-

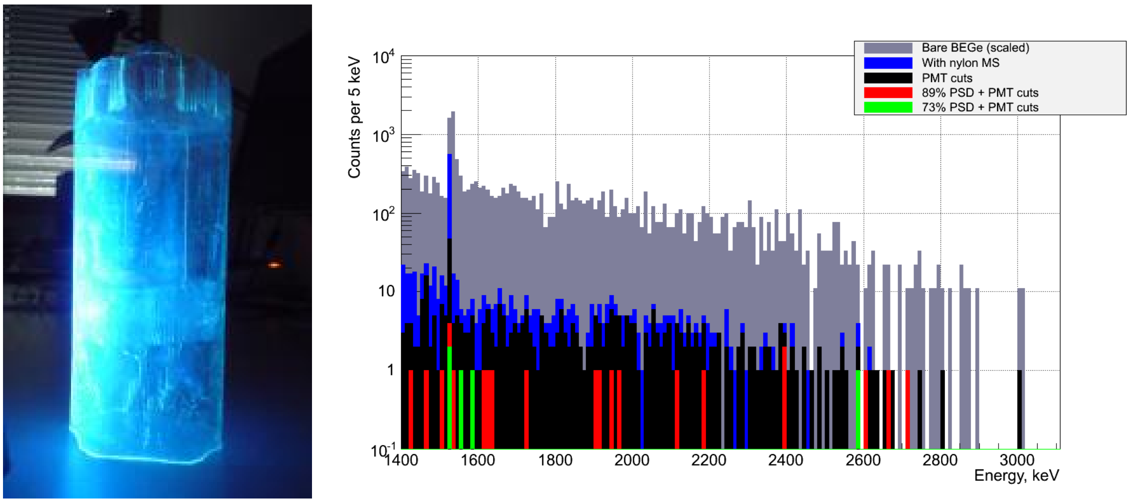

Figure 6: Left: Nylon foil covered with TPB; illuminated with a UV lamp. Right: ^{42}K background suppression studies in LArGe: without suppression (grey), with nylon shroud (blue), with additional LAr veto (black), with additional pulse shape discrimination PSD (red and green).

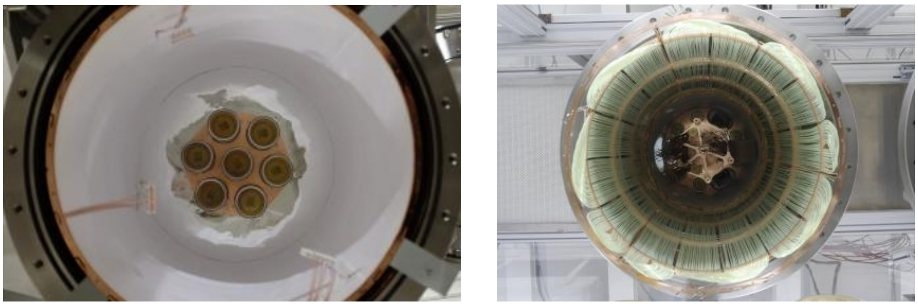

Figure 7: Pictures from the Liquid Argon veto instrumentation. Left: view inside the copper cylinder covered with Tyvek and the bottom PMTs. Right: central view of the fiber curtain, part of the detector suspension mechanics in the middle and the top PMT plate.

tillation cut only and, finally, the suppressed spectrum after both PSD plus LAr scintillation cut. The total suppression factor is about a factor 50 for the LAr veto alone and 90 for the combined selection. Since only half of the SiPM channels worked properly in the first installation we expect an even higher suppression factor in the configuration with the full equipment. Recently, all broken SiPM channels have been replaced with new ones having better quantum efficiency.

5. Conclusions

First commissioning results show that the expcted background foreseen for GERDA Phase II can be achieved. Considering a background index BI$\simeq 10^{-3}$ cts/(keV·kg·yr) and an exposure of 100 kg·yr (corresponding to about 3 years of data taking), the projected sensitivity for the half-life of neutrinoless double beta decay is $T^{0\nu}_{1/2} > 1.4 \cdot 10^{26}$ yr.

PoS(NEUTEL2015)050

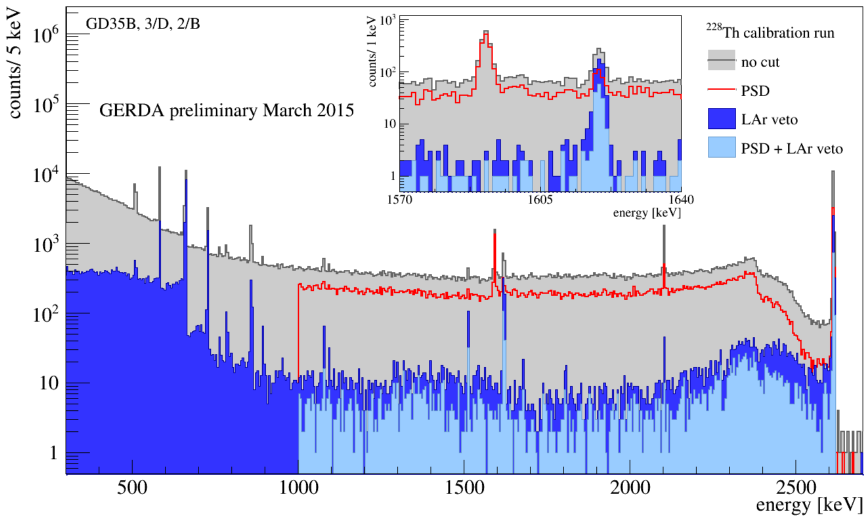

Figure 8: ^{228}Th calibration spectrum (filled grey histogram) after pulse shape discrimination (PSD, red curve), after the liquid argon veto is applied (LAr veto, filled dark blue histogram) and the combination (PSD + LAr veto, filled light blue histogram). The insert shows the double escape peak at 1592 keV which is only rejected by the LAr veto and the ^{212}Bi line at 1621 keV which is mainly suppressed by PSD (by the LAr veto only due to random coincidences of two decays).

References

[1] The GERDA collaboration, *Eur. Phys. J. C* **73**, (2013) 2330.

[2] M. Agostini et al., *J. Instrum.* **6**, (2011) P08013.

[3] The GERDA collaboration, *Eur. Phys. J. C* **74**, 276 (2014).

[4] The GERDA collaboration, *Eur. Phys. J. C* **73**, 2583 (2013).

[5] The GERDA collaboration, *Phys. Rev. Lett.* **111**, 122503 (2013).

[6] C. Macolino on behalf of the GERDA collaboration, *Mod. Phys. Lett. A* **29**, 1430001 (2014).

[7] H.V. Klapdor-Kleingrothaus et al., *Phys. Lett. B* **586**, 198 (2004).

[8] H.V. Klapdor-Kleingrothaus et al., *Eur. Phys. J. A* **12**, 147 (2001).

[9] C.E. Alseth et al., *Phys. Rev. D* **65**, 092007 (2002).

[10] The GERDA collaboration, submitted to *Eur. J. Phys. C*. [arXiv:1501.02345].

[11] The GERDA collaboration, submitted to *J. Phys. G: Nucl. Phys.*. [arXiv:1506.03120v1].

[12] M. O. Deighton, *IEEE Trans. Nucl. Sci.* **16** 68 (1969).

[13] A. Geraci et al., *Nucl. Instrum. Methods A* **482** 441 (2002).

[14] The GERDA collaboration, accepted for publication in *Eur. Phys. J. C*. [arXiv:1502.04392].

[15] The GERDA collaboration, *Eur. Phys J. C* **75** 39 (2015).

[16] T. Goldbrunner, Dissertation *Technische Universtät München*, 1997.

[17] L. Cadonati et al, *Int. J. Mod. Phys. A* **29** 1442004 (2014).

[18] M. Agostini et al, submitted to *Eur. Phys. J. C*. [arXiv:1501.05762].